Astronomy & Astrophysics

Interactions, mergers and the fundamental mass relations of galaxies

P. B. Tissera[1,2], A. V. Smith Castelli[1,3], and C. Scannapieco[1,2]

[1] Consejo Nacional de Investigaciones Científicas y Técnicas, Argentina
  e-mail: patricia@iafe.uba.ar
[2] Instituto de Astronomía y Física del Espacio, Argentina
[3] Facultad de Ciencias Astronómicas y Geofísicas, La Plata, Argentina

ABSTRACT

We present a study of the effects of mergers and interactions on the mass distribution of galactic systems in hierarchical clustering scenarios using the disc-bulge structural parameters and their dynamical properties to quantify them. We focus on the analysis of the Fundamental Mass Plane relation, finding that secular evolution phases contribute significantly to the determination of a plane with a slope in agreement to that of the observed luminosity relation. In these simulations, secular phases are responsible for the formation of compact stellar bulges with the correct structural parameter combination. We also test that the relations among these parameters agree with observations. The Kormendy mass relation is also reproduced after secular evolution phases. From our findings, we predict that the departure of systems from the $z = 0$ Fundamental Mass Plane, involving a change in the slope, could indicate a lack of secular evolution in their formation histories. Taking into account these results, the hierarchical growth of the structure predicts a bulge formation scenario for typical field spiral galaxies where secular evolution during dissipate mergers plays a fundamental role. Conversely, subsequent mergers can help to enlarge the bulges but do not seem to strongly modify their fundamental mass relations. Systems get to the local mass relations at different stages of evolution (i.e. different redshifts) so that their formation histories introduce a natural scatter in the relations. We also found that the parameters of the Tully-Fisher Mass relation for the disc components are correlated with those of the Fundamental mass one for the bulge components at least during mergers events, so that as the systems increase their circular velocity, the bulges get more concentrated. Our results suggest that the formation mechanisms of the bulge and disc components, satisfying their corresponding fundamental mass relations, might be coupled and that secular evolution could be the possible connecting process.

Key words. galaxies: structure – galaxies: interactions – galaxies: fundamental parameters

1. Introduction

The origin of the fundamental relations of galaxies such as the Tully-Fisher (TF) for spiral galaxies and the Fundamental Plane (FP) for ellipticals and early-type bulges, is still under discussion. Although, assuming the virialization of the systems, the main features of both relations can be explained within a hierarchical scenario, mergers and interactions redistribute mass and angular momentum in galaxies and, as a consequence, they can affect the relation between their structural and dynamical parameters.

The simplest scenarios currently accepted for the formation of bulges in disc galaxies are two: the first one establishes that the bulge and the disc are formed independently, the bulge being formed previously to the disc (Andredakis et al. 1995); the second scenario assumes that the disc forms first and, the bulge emerges from it as a consequence of gas inflows during a period of secular evolution (Courteau et al. 1996). Within hierarchical clustering scenarios, bulges have been modeled through the merger of smaller systems (e.g. White & Rees 1978; Cole et al. 2000). However, it is still a matter of debate which are the main physical mechanisms involved in the formation of bulges and at what extent they are coupled to the formation of the disc component.

Observationally, several works have considered to this problem. By applying a bulge-disc decomposition with a Sérsic profile to bulges, Andredakis et al. (1995) found that the Sérsic index n varies in a continuous and smooth way from values $n \approx 1$ for late-type bulges, to values $n \approx 6$ for early-type bulges. As a consequence, the authors argued that all bulges formed by a common mechanism (see also Bender et al. 1992; Khoroshahi et al. 2000a,b; Möllenhoff & Heidt 2001). However, Courteau et al. (1996) suggested that such a smooth sequence could be the result of a scenario in which early-type bulges emerged from a minor merger, and late-type bulges formed via secular evolution, both processes operating to some degree of efficiency for all Hubble types.

The formation of disc systems is well-explained by assuming the conservation of the specific angular momentum of the baryonic component as it collapses onto the dark matter potential well of the system (Fall & Efstathiou 1980; White & Rees 1978). This simple scheme has served as a basis to build more complex models for galaxy formation (e.g. Lacey et al. 1993; Mo et al. 1998), which have been successful in reproducing several observational results, but which have the shortcoming of not being able to self-consistently describe the effects of mergers and interactions, ubiquitous in the current cosmological paradigm.

In fact, if the structure forms in a hierarchical scenario, mergers play an important role in the formation of galaxies and, as a consequence, in the determination of their properties and fundamental relations. Numerical simulations remain a useful tool to study galaxy formation in a cosmological context. Regarding the FP relation of spheroids, Capelato et al. (1995) and Evstigneeva et al. (2003) have investigated the effects of mergers by using pure N-body numerical simulations. Recently, Kobayashi (2005) studied the formation of elliptical galaxies in cosmological simulations, finding that the different merger histories of the systems introduced an important scatter in their FP relation.

The formation of disc systems in hierarchical scenarios have been studied by several authors. In particular, Scannapieco & Tissera (2003, hereafter ST03) studied the effects of mergers on the structural properties of disc-like systems by using smooth particle hydrodynamical (SPH) numerical simulations. These authors focused on the analysis of the mass distributions of disc-like objects and how they are modified during mergers. In this work, a comparative study of the effects of secular evolution triggered by tidal fields and of the actual collision of the baryonic clumps was carried out. ST03 found that galactic objects formed in hierarchical clustering scenarios reproduce the angular momentum and structural parameter distributions of spiral galaxies, if a stellar compact bulge is allowed to form and early gas depletion is avoided. The formation of a compact stellar bulge provides stability to the cold gaseous discs (Athanassoula & Sellwood 1986; Binney & Tremaine 1987; Barnes & Hernquist 1991, 1992; Martinet 1995 and references therein; Mihos & Hernquist 1994, 1996; Mo et al. 1998), preventing the triggering of non-axisymmetric instabilities by interactions and mergers (Christodoulou et al. 1995; van den Bosch 1998, 2000). The latter can cause important angular momentum losses followed by strong gas inflow (Navarro & Benz 1991; Navarro et al. 1995a,b; Evrard et al. 1994; Vedel et al. 1994; Navarro & Steinmetz 1997; Sommer-Larsen et al. 1999; Weil et al. 1998). By adopting an artificial low efficiency for the star formation activity, ST03 (see also Domínguez-Tenreiro et al. 1998 and Sáiz et al. 2001) were able to avoid the formation of too-concentrated, pure gaseous discs (e.g. Navarro & Benz 1991; Navarro et al. 1995a,b; Evrard et al. 1994) or a stellar spheroid-dominated system (e.g. Thacker & Couchman 2000). Supernova energy feedback should provide a self-consistent regulation of the star formation activity, allowing the formation of extended discs. However, a self-consistent SN feedback model within SPH has not been yet presented (see Scannapieco et al. 2006 for a new promising approach).

In this paper, we will continue the analysis of ST03, investigating other structural parameters and, particularly, the FP relation, with the aim of analyzing how mergers change the mass distribution and the fundamental relations. Contrary to pre-prepared mergers, we use fully self-consistent, cosmological hydrodynamical simulations, where the distribution of merger parameters and the physical characteristics of the interacting systems arise naturally at *each epoch* as a consequence of working within a cosmological scenario. No ad hoc set of orbital parameters or dynamical characteristics for the galactic systems need to be assumed in this work. The effects of mergers and interactions on star formation can be studied in a consistent scenario, although at the expenses of losing numerical resolution.

This paper is organized as follows. In Sect. 2 we give a summary of the simulations and method used by ST03 to determine the structural parameters. In Sect. 3 we discuss the results and compare them with observations. Section 4 summarizes the results.

2. Numerical experiments

The simulations used in this paper have been analyzed by Domínguez-Tenreiro et al. (1998), Tissera (2000), Sáiz et al. (2001), Tissera et al. (2002), and ST03. These simulations are consistent with a standard Cold Dark Matter ($\Omega = 1$, $\Lambda = 0$, $H_0 = 100$ km s^{-1} Mpc^{-1} h^{-1} with $h = 0.5$) universe and represent a 5 h^{-1} Mpc side box using 64^3 particles. The gravitational softening adopted is 1.5 kpc h^{-1}, and the minimum hydrodynamical smoothing length is 0.75 kpc h^{-1}. A baryonic density parameter of $\Omega_b = 0.10$ is assumed. All baryonic and dark matter particles have the same mass, $M_p = 2.6 \times 10^8$ $M_\odot$. The three realizations of the power spectrum (cluster normalized) were run by using the SPH code of Tissera et al. (1997), which includes radiative cooling and star formation (hereafter, main runs). In this paper, we also analyzed three typical galactic systems in a high resolution run performed with Gadget-2 (Sect. 2.3) to assess possible numerical effects.

The size of the simulated volume is the result of a compromise between the need to have a well-represented galaxy sample and enough numerical resolution to study the astrophysical properties of the simulated galaxies. We are confident that since we focus our analysis on small-scale processes such as mergers and interactions, scale fluctuations of the order of the box size will have no significant effect on such local processes. Moreover, since we are interested in the possible changes triggered by galaxy-galaxy interactions, the results are also weakly dependent on the detailed cosmological parameters adopted (see also Pérez et al. 2006). In this work, we aim to understand the physical processes at work during mergers and not to probe the cosmological model itself. As we mentioned before, we focus this study on the effects that mergers have on the mass distributions of the galactic objects, analysing them as individual events and not in connection with their history of evolution or environment.

The star formation algorithm used in these models is based on the Schmidt law and transforms cold and dense gas particles into stars if they are denser than a certain critical value and satisfy the Jeans instability criterion (Navarro & White 1994). Gas particles are checked to satisfy these conditions at all time-steps of integration. Then, as the gas cools down and accretes onto the potential wells of dark matter halos, it is gradually transformed into stars. The star formation timescale of a given gas particle is assumed to be proportional to its dynamical time by adopting a star formation efficiency parameter. This parameter is the only free one in these models and has been kept constant in all analyzed simulations.

The star formation efficiency used in these simulations is the one adopted by Sáiz et al. (2001), since it is adequate to reproduce disc-like structures with observational counterparts at $z = 0$. These authors used a low star formation efficiency which allows the formation of stellar bulges that assure the axisymmetrical character of the potential well, but without exhausting the gas reservoir of these systems (see also Domínguez-Tenreiro et al. 1998). As a consequence, disc-like structures can be formed, although they remain mainly gaseous. If the star formation process continued normally, the gaseous discs would be transformed into stars. These stars would inherit the dynamical and astrophysical properties of their progenitor gas clouds. Hence, we assume that structural properties of the gaseous discs reflect those of the stellar discs that formed out of them. In this paper, we will determine and use these parameters to study the effects of mergers on the mass distribution of the simulated galactic objects and the fundamental relations they define.

2.1. Merger events and bulge-disc decompositions

We used the set of merger events studied by ST03. These authors identified galactic objects at their virial radius, analyzing only those with more than 4000 total particles at $z = 0$ within their virial radius to diminish numerical resolution problems. Within each galactic object, a main baryonic clump is individualized, which will be, hereafter, called the galaxy-like object (GLO).

The selected GLOs have very well-resolved dark matter halos which provide adequate potential wells for baryons to collapse in. This fact assures a reliable description of the gas density profiles (see Steinmetz & White 1997), which allows us to follow the star formation history of the GLOs (see Tissera 2000). With this strong restriction on the minimum number of particles, the final GLO sample at $z = 0$ is made up of 12 GLOs with virial velocities in the range 140–180 km s^{-1}. These systems spawned from $z = 0$ to $z \approx 1.5$, as shown by ST03.

ST03 followed the evolution of the selected GLOs back in time, constructing their merger trees and star formation rate (SFR) histories. Then mergers and starbursts (SBs) were identified. In this paper, we worked with the same set of GLOs and merger events analyzed by ST03. The latter are classified taking into account the SF activity taking place during the mergers. During a merger event, the progenitor object is chosen as the more massive baryonic clump within this merger tree, while the minor colliding baryonic clump is referred to as the satellite. If no gas inflows are induced during the orbital decay phase (ODP), then only one SB is triggered when the two baryonic clumps collide. These events are cataloged as single SBs (SSBs). If the system is unstable and tidal torques are able to drive instabilities inducing early gas inflows during the ODP, then two SBs are detected, one associated with the ODP and the second one with the actual collision. These events are classified as double SBs (DSBs). The total set of events compromises 18 mergers with orbital and dynamical parameters settled by the cosmological model. Among them, 11 are classified as DSBs and 7 as SSBs.

Merger events are characterized by four redshifts of reference; z_A: the beginning of the first bursts in DSBs and the ODP in SSBs, z_B: the end of both the first bursts in DSBs and the ODP in SSBs, z_C: the beginning of the second SBs in DSBs and the only bursts in SSBs (in this case $z_B = z_C$), and z_D: the end of the second bursts in DSBs and of the only one in SSBs. It is important to stress that the ODP phase is determined by z_A and z_C. These two redshifts determined the time elapsed since two objects share the same dark matter halo until the fusion of their main baryonic cores. The z_B redshift is only used in the case of DSBs to measure the end of the first SBs.

We used the structural parameters calculated by ST03, who carried out a bulge-disc decomposition of the integrated projected baryonic mass surface density of the GLOs at $z = 0$ and of the progenitors at each of the redshifts that define a merger event (z_A, z_B, z_C, and z_D). The projections were carried out on the plane perpendicular to the total angular momentum of the systems. ST03 followed the procedure explained in detail by Sáiz et al. (2001). ST03 adopted the Sérsic law (Sérsic 1968) for the bulge central mass concentration and an exponential for the disc. As discussed in Sáiz et al. (2001), it is more robust to perform the fitting of the integrated mass density distributions since they are not binning-dependent and are less noisy than the density profiles.

Note that in numerical studies it is mass density distributions and not the luminosity density profiles which are analyzed. In this work we are interested in the the changes in the mass distribution during mergers but for the sake of comparison with observations we need to assume mass-to-light ratios. We adopt a disc mass-to-light ratio $\Gamma = 7$ regardless of redshift, disc scale-lenghts and observational band and a ratio between the disc and the bulge mass-to-light ratios of 20 to be consistent with the analysis of ST03. The combination of these mass-to-light ratios provides a good fit to the fundamental relations. Note, however, that we are using the total baryonic masses to estimate luminosities (due to our low star formation efficiency). In a more realistic model including Supernova feedback a fraction of this mass should be heated up and even expelled from the systems. Hence, the adopted mass-to-light ratios should be considered only as upper limits.

We carried out 75 disc-bulge decompositions (see Sáiz et al. 2001 and ST03 for details of the procedure and error discussion). The baryonic mass and the circular velocity ($V_{2.2}$) are measured at $2.2r_d$. The analyzed systems can be classified as intermediate spirals (100 km s^{-1} < $V_{2.2}$ < 180 km s^{-1}, 46 systems), late spirals ($V_{2.2}$ > 180 km s^{-1} and r_d > 5.25 kpc, 6 systems), or compact spirals ($V_{2.2}$ > 180 km s^{-1} and r_d < 5.25 kpc, 23 systems). Because of our minimum required number of particles, we do not have any dwarf galaxies in this sample.

2.2. Observational data for comparison

Since in these simulations we are analyzing the properties of the mass distributions, the confrontation of the results with observational data is not direct. While observations provide information on luminosity density distributions, our analysis will give us insight into the mass properties that are not affected by dust or stellar evolution. However, we would like to compare our findings with observations, and to this end, we assume mass-to-light ratios for the bulge and for the disc components to match the fundamental relations at $z = 0$. But the reader should bare in mind that the comparison with observations is made in broad terms.

We compiled observations from different authors who analyzed the brightness surface density profiles (re-scaled to $H_0 = 50$ km s^{-1} Mpc^{-1}) by using the Sérsic law to fit the bulge brightness distribution. For the structural parameters, we used the data from Khosroshahi et al. 2000b (K00b) which include 26 early- to intermediate-type spirals in the K-band. These authors used the same software packages that we applied in this work to perform the bulge-disc fittings (i.e. MINUIT). For the luminosity FP, we adopted the derived by Falcón-Barroso et al. (2002, hereafter FBPB02) from 19 S0-Sbc bulges in the K-band. Note that all these observations correspond to galaxies at $z \approx 0$. Unfortunately, we do not have a unique set of observed parameters to confront the structural parameters and the fundamental plane.

2.3. Numerical resolution

Regarding numerical resolution, in the main runs, the baryonic components of galaxy-like systems are resolved with a relatively low number of particles. In contrast, dark matter halos are described with a much better resolution. An inappropriate low gas resolution would result in a nonphysical gas heating that could halt the gas collapse. In fact, some works suggest that it is an inadequate resolution in the dark matter halo component that may produce the larger numerical artifacts (Steinmetz & White 1997). In fact, it appears that a well-resolved dark matter halo, no matter if the number of gas particles is low (although larger than 500 gas particles), gives rise to a well-represented gas density profile, this being the most important point for both the

hydrodynamics and the tracking of the star formation history. Domínguez et al. (1998) have already proved that it is possible to reproduce populated and extended discs in high resolution simulations of standard CDM scenarios.

In this paper, we carried out a high resolution simulation by using 2×64^3 total particles (hereafter HR) with a chemical Gadget-2 (Scannapieco et al. 2005), adopting *the same cosmology and initial conditions of one of our main runs* (i.e., the parameters of the high resolution simulation are the same listed in Sect. 2 for the main runs, except for the particle masses). Dark matter is resolved with the same number of particles (i.e. 64^3) in the main and high resolution runs, but the baryonic resolution is improved by one order of magnitude in the HR experiment (i.e. 64^3). The star formation efficiency was set, as we did in the main runs, so that stars formed only in the very high density regions. In this way, compact stellar cores are allowed to form without exhausting the gas reservoir at early stages of evolution (Domínguez et al. 1998; ST03). The bulge/disc parameters obtained for the high resolution systems are consistent with the relations obtained from the lower resolution run.

It deserves to be stressed that the high resolution run is performed with a different code, Gadget-2, which has been improved to conserve entropy when appropriate and includes chemical evolution and metal-dependent cooling. Hence, the fact the galactic systems follow the trends obtained for those in our main runs provides strong support to our findings.

3. Results

In this section, we assess the structural parameters of the simulated bulges and the discs and the fundamental relations they determine during merger events and at $z = 0$. We have adopted a mass-to-light ratio in order to confront the results with observations. But, we are mainly interested in the mass redistribution during merger events and how that affects possible correlations. Furthermore, the correct estimations of luminosities would imply the treatment of other physical processes such as SN energy and metallicity feedback which are beyond the scope of this work.

3.1. Correlations among structural parameters

In this section we focus only on the analysis of the structural parameters of the bulges and the relation with those of the discs, since Domínguez et al. (1998), Sáiz et al. (2001), Tissera et al. (2002), and ST03 had exhaustively studied the properties of disclike structures. In these works, the simulated GLOs were found to have bulge and disc scale lengths comparable to those of spiral galaxies and to show the expected relation with the shape parameter n, as discussed by ST03. In Fig. 1, we show the ratio between the bulge and the disc scale lengths (r_b, r_d) of the simulated objects as a function of the shape parameter (Fig. 9 in ST03). We have included the values for the GLOs analyzed in the HR test, which are found to be consistent with the relation determined by the main runs.

We have investigated possible correlations between the shape parameter n and the structural parameters, finding only a signal of anti-correlation with Σ_b^o, as shown in Fig. 2 (see also Table 1). It is interesting to note that the simulated bulges yield the same slope for this relation independently of the redshift. In Fig. 2 we have also included the observations from K00b which include early and intermediate spirals. We can appreciate a slight offset between simulations and observations which could be due
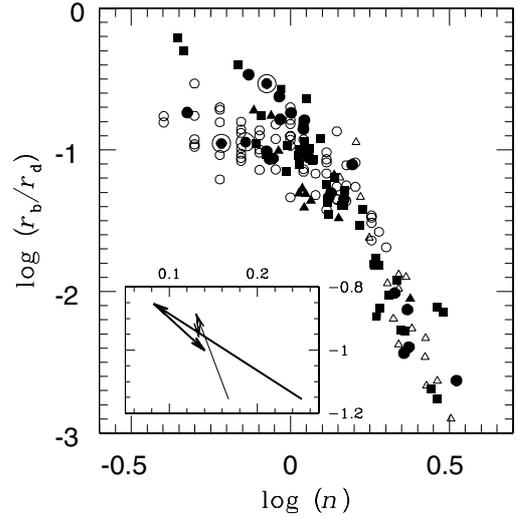
Fig. 1. Ratio between bulge and disc scale lengths as a function of the bulge shape parameter for simulated objects at $z = 0$ (filled triangles), single SBs (filled circles), and double ones (filled squares). Filled circles in open circles correspond to the parameters for the high resolution systems. Observational data from Khosroshahi et al. (2000b; open triangles) and MacArthur et al. (2003; open circles) are also shown. The small box shows the changes of the plotted parameters for single (solid thin line) and double (solid thick line) SBs during the orbital decay phase (first arrow) and the fusion of the baryonic clumps (second arrow).
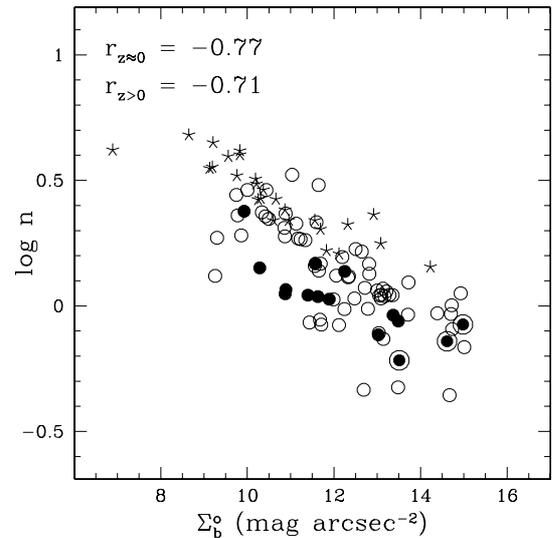
Fig. 2. log n as a function of Σ_b^o for simulated bulges at $z \leq 0.03$ (filled circles) and $z > 0.03$ (open circles). Filled circles in open circles correspond to the parameters for the high resolution systems. We have included the correlation coefficients. The observational data from Khosrhoshahi et al. (2000b, stars) are also displayed for comparison.

to the fact that we are using a fixed mass-to-light ratio and total baryonic masses to estimate surface brightness. The HR systems are consistent with the trend determined by GLOs in the main runs (for the HR systems, we assume the same mass-to-light ratios used in the main runs).

In Fig. 3, we show the bulge effective surface density (Σ_{eff}) as a function of the effective radius (r_{eff}) for all simulated objects at all studied redshifts and for the HR systems. We used the relation given by MacArthur et al. (2003) to derive Σ_{eff} and r_{eff}. To carry out a more thoughtful analysis, we performed linear

Table 1. Correlations between mass structural parameters.

	Σ_{eff} vs. Log r_{eff}		$\Sigma_{\text{d}}^{\text{o}}$ vs. Log r_{d}		Log n vs. $\Sigma_{\text{b}}^{\text{o}}$		
	a	r	a	r	a	r	[a]
Sim($z = 0$)	0.13 ± 0.01	0.94	0.13 ± 0.02	0.92	-0.09 ± 0.02	-0.77	
Sim($z > 0$)	0.15 ± 0.01	0.90	0.14 ± 0.01	0.91	-0.10 ± 0.01	-0.71	
K00b	0.15 ± 0.05	0.52	0.24 ± 0.06	0.65	-0.08 ± 0.01	-0.88	

[a] Slopes of linear regressions ($y = ax + b$) and Pearson linear correlation coefficients for the simulated galaxy-like objects at $z = 0$ (Sim($z = 0$)), for their progenitors during merger events (Sim($z > 0$)), and the observed bulges and discs of Khosrhoshahi et al. (2000b).
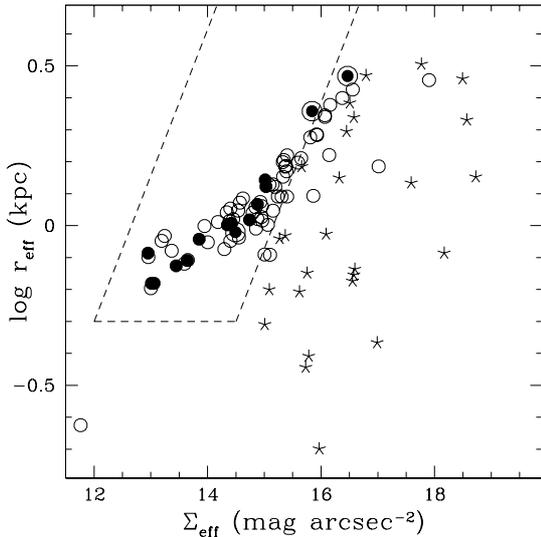
Fig. 3. Bulge effective surface density (Σ_{eff}) as a function of the effective radius (r_{eff}), for simulated objects at $z \leq 0.03$ (filled circles) and $z > 0.03$ (open circles). Filled circles in open circles correspond to the parameters for the high resolution systems at $z = 0$. Observational data from Khosrhoshahi et al. (2000b, stars) are shown for comparison. We also depicted the region occupied by ellipticals from Khosrhoshahi et al. (2000a).

regressions through the data and the observations. In Table 1 we show the slopes of the fits and the corresponding Pearson linear correlation coefficient, r. As it can be appreciated, there are clear correlation signals between the simulated structural parameters of the bulges (log r_{eff} vs. Σ_{eff}) of galaxy-like objects at $z \approx 0$ and for their progenitors ($z > 0$). We found that the slope of the simulated relation at $z = 0$ agrees with the one derived from K00b within the observed dispersion. The same is valid for the relation estimated for the simulated bulges at $z > 0$, although, in this case, we note a change in the slope for small r_{eff}. We will come back to this point in Sect. 3.2 The fact that these simulated parameters for the bulges show a tighter relation that that of Fig. 2 is produced by their definations, which are coupled through the a shape parmeters n. In the case of n and $\Sigma_{\text{b}}^{\text{o}}$, they are both estimated from the bulge-disc decomposition as independent parameters (see ST03 for details). As mentioned before, the displacement between the simulated bulges and the K00b could be due to the fact that we are using a constant mass-to-light ratio for all bulges at all analyzed redshifts. The fact that the simulated bulges are displaced toward the elliptical regions could indicate that, in these simulations, we tend to reproduce mainly large bulges. A wider range of bulges is expected to be given if Supernova energy feedback is correctly implemented. However, there is currently no consistent Supernova feedback implementation in SPH (see Scannapieco et al. 2006 and Tissera et al. 2006

for a promising approach). In Table 1, we also included the corresponding linear fits for disc structural parameters, log r_{d} vs. $\Sigma_{\text{d}}^{\text{o}}$, which also show a good agreement with observations.

3.2. The Fundamental Mass Plane for simulated bulges

As it was discussed in the Introduction, it is not yet clear if bulges determine the same FP of elliptical galaxies. In this section, we investigate if the simulated bulges at $z = 0$ satisfy a FP mass relation.

For that purpose, we adopt the luminosity FP determined by FBPB02 for Coma cluster ellipticals and early-type spiral bulges as a reference plane:

$$FPR = 1.3 \cdot \log \sigma_0 + 0.3 \cdot \Sigma_{\text{eff}} - 7.31, \qquad (1)$$

where σ_0 is in km s^{-1} and Σ_{eff} is in mag arcsec^{-2}.

We assume the circular velocity ($V^2 = GM/(r^2 + \epsilon_g^2)^{3/2}$, where ϵ_g is the gravitation softening) at 2 kpc h^{-1} as an estimate of the depth of the potential well and central velocity dispersion (σ_0). As we have already mentioned, the effective surface brightness (Σ_{eff}) is obtained following McArthur et al. (2003) from n and $\Sigma_{\text{b}}^{\text{o}}$. We acknowledge that the mass-to-light ratio can change with luminosity and redshift, among other things. However, we keep it constant, so that *deviations from the mass FP can be directly linked to differences in mass distributions and velocity patterns*, and not to stellar population evolution or dust effects.

In Fig. 4, we show the FP of the simulated bulges at $z = 0$ and their progenitors during merger events. We have also included the region occupied by ellipticals taken from FBPB02. As expected, the simulated bulges populate the smaller r_{eff} extreme, and at $z = 0$, they show a slope and scatter in agreement with observations. Their progenitor systems at $z > 0$ tend to be above the $z = 0$ relation.

The HR systems follow the same FP mass relation and require the same mass-to-light ratios to match the observations. We claim that if systems at $z = 0$ have structural parameters and reproduce a fundamental plane in agreement to those of the main runs, then their evolutionary history during mergers would be statistically similar. Hence, for the sake of simplicity, we only include calculations for the HR systems in the analysis at $z = 0$.

3.2.1. The effects of mergers

In this section, we will focus on the analysis of the effects of mergers on the FP mass relation by studying mergers during two phases: orbital decay and fusion phases. In this way, we will try to individualize the effects of secular evolution and collision. The merger events analyzed here are those studied by ST03, as was mentioned in Sect. 2.2.

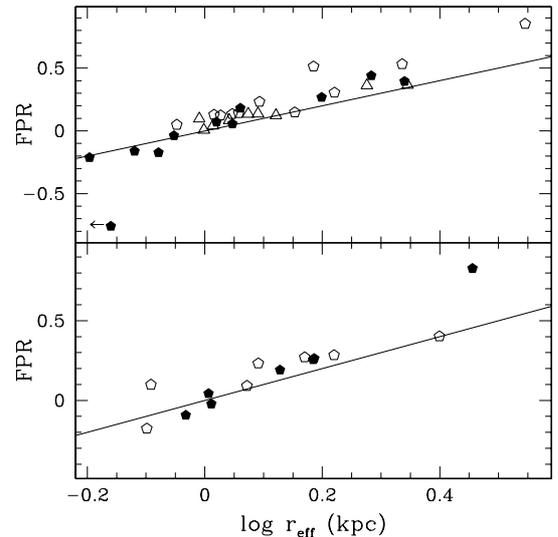**Table 2.** Mean variation in structural parameters and FP residuals.

	ΔFP		Δr_{eff}		$\Delta \Sigma_{eff}$		$\Delta \sigma_0$		Δn		$\Delta M_b{}^a$	
	ODP	Fusion	ODP	Fusion	ODP	Fusion	ODP	Fusion	ODP	Fusion	ODP	Fusion
DSBs	−0.09	0.03	−0.26	−0.14	0.46	−1.02	25.6	25.1	−0.57	0.17	1.15	1.25
Errors	0.03	0.01	0.12	0.10	0.53	0.33	6.97	6.10	0.22	0.21	0.42	0.44
SSBs	−0.01	0.03	0.05	0.03	0.28	0.02	−3.93	8.99	−0.12	0.01	−0.10	−0.11
Errors	0.01	0.05	0.03	0.04	0.19	0.83	0.90	7.72	0.10	0.47	0.23	0.56

^{a} Statistical errors estimated by applying the bootstrap technique are given within parenthesis.
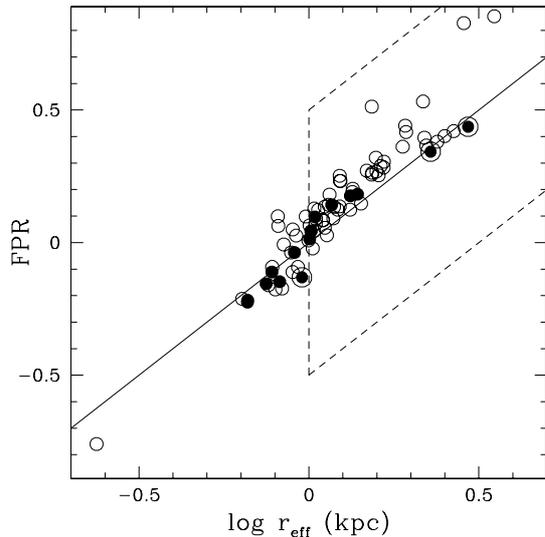
Fig. 4. The simulated fundamental mass plane for bulges at $z \approx 0$ (filled circles) and their progenitors during merger events (open circles). For the sake of confrontation, constant mass-to-light ratios for the bulge and the disc components have been assumed by requiring the $z = 0$ systems to match observations. Encircled filled circles correspond to the parameters for the high resolution systems. The observed FP of FBPB02 (solid line) and the region occupied by ellipticals (dashed rectangle) have been also depicted.

Fig. 5. FP for simulated bulges undergoing double starburst (*upper panel*) events at z_A (open pentagons), z_C (open triangles), and z_D (filled pentagons), and single starburst events (*lower panels*) at z_A (open pentagons) and z_D (filled pentagons). The observed FP of FBPB02 (solid line) has been included. The pentagon with the arrow depicts a point that, for the sake of clarity, has been artifially displaced from its original position at log $r_{eff} = -0.62$.

In Fig. 5, we show the mass FP relations for systems at double and single SB events. The upper panel shows the mass FP at the three, defined stages of the so-called double SB events. As it can be clearly seen, bulges at z_A (open pentagons), although being ordered, are all displaced to higher values than those of the observed FP at $z = 0$ (solid line). After the secular evolution period (open triangles), bulges are located more closely to the observed relation. Fusions (filled pentagons) contribute to scatter the objects along this relation. When the systems experience single SB events (lower panel), their bulge components, on average, already show a FP mass relation with a slope in good agreement with observations at the beginning of the merger (open pentagons). The fusions do not seem to strongly modify the slope (filled pentagons). We note, however, that one point is located considerably far away from the relation after fusion. This system has not been detected as one that experiences early gas inflows during the ODP, but it is gas-rich and transforms an important fraction of its gas mass into stars during the fusion. Since we are considering a variety of merging systems from cosmological simulations, we expect not all the systems to follow exactly the same patterns. An analysis of a larger set of mergers with higher numerical and temporal resolution could show if the particular evolutionary path of this system is statistically significant.

To quantify the changes in FP relations during merger events, we followed FBPB02 and defined the residuals ΔFP along the x-axis by:

$$\Delta FP = (\log r_{eff})_{sim} - (\log r_{eff})_{obs}, \qquad (2)$$

where $(\log r_{eff})_{sim}$ and $(\log r_{eff})_{obs}$ are the effective radius estimated from the simulated bulge-disc decomposition and from the observed FP relation, respectively.

The assessment of the effective changes in ΔFP during the two main periods in a merger event (i.e., ODP and fusion) was done by calculating the difference between the absolute values of the residuals during the orbital decay phase (i.e., $\Delta FP(z_C)$ and $\Delta FP(z_A)$) and during the fusion itself (i.e., $\Delta FP(z_D)$ and $\Delta FP(z_C)$; for simplicity we assume $z_B = z_C$) as a function of the variation in the structural parameters. We aim to detect if the net effect of the events is to strengthen the FP relation or to dilute it by increasing the residuals. Recall that double starbursts are produced by secular evolution induced by the lack of well-formed bulges that could provide stability to the discs (Tissera et al. 2002). Hence, this separation in SSBs and DSBs can be interpreted as a classification of systems according to the properties of their potential well.

As it can be appreciated from Table 2, those systems which experience SSBs events do not significantly vary their structural parameters or their residual ΔFP during the ODPs. Errors have
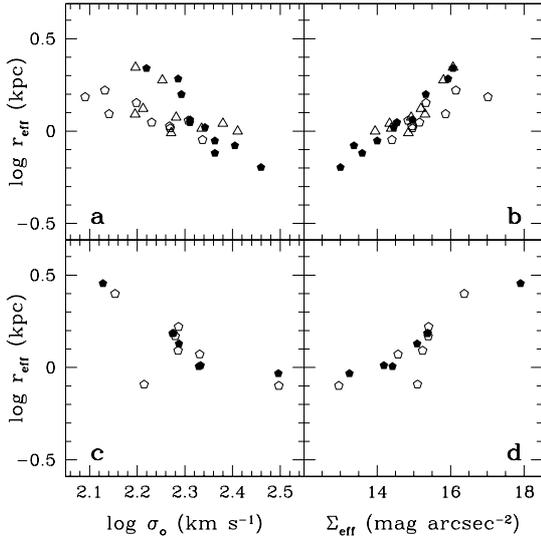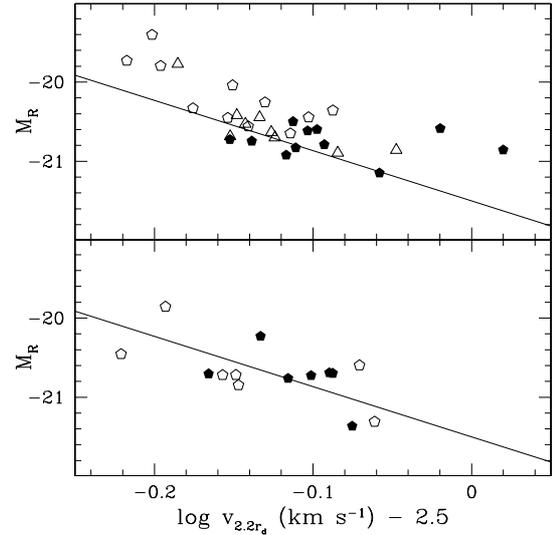
Fig. 6. log($r_{\rm eff}$) as a function of log(σ_0) **a)**, **c)** and $\Sigma_{\rm eff}$ **b)**, **d)**. Figures **a)**, **b)** show the relations for the objects that experience double starburst events; meanwhile, figures **c)**, **d)** correspond to the systems that present single starburst events. In all cases, open pentagons correspond to $z_{\rm A}$, open triangles to $z_{\rm C}$, and filled pentagons to $z_{\rm D}$.

Fig. 7. Tully-Fisher relation for simulated bulges undergoing double starburst (DS) events (*upper panel*) at $z_{\rm A}$ (open pentagons), $z_{\rm C}$ (open triangles), and $z_{\rm D}$ (filled pentagons) and single starburst (SS) events (*lower panels*) at $z_{\rm A}$ (open pentagons) and $z_{\rm D}$ (filled pentagons). The solid line represents a linear regression fit to the observational data of MacArthur et al. (2003).

been calculated by applying the bootstrap technique which provides a more reliable statistical estimation of numerical noise due to low statistical number. The variations in the residuals of the Fundamental Mass Plane are within a σ level for these systems where a well-formed bulge is present (i.e., $\Delta FP = -0.01 \pm 0.01$ during the ODP and $\Delta FP = 0.03 \pm 0.05$ during the fusion), confirming that these objects are stable during interactions and their mass distributions are not significantly altered during the secular evolution phase or in the fusion itself. The structural parameters of these systems remain statistically unchanged.

In those systems which undergo DSBs events, secular evolution tends to reduce the residuals at a 3σ level ($\Delta FP = -0.09 \pm 0.03$), while the fusion itself increases the dispersion also at a 3σ level ($\Delta FP = -0.03 \pm 0.01$). However, in absolute terms, secular evolution has a larger effect and contributes to tighten the relation. From the analysis of the variation of the structural parameters of these systems, we found that secular evolution helps to build up the bulge component and to make it more exponential with a change in the mean n shape parameter of $\Delta n = -0.57 \pm 0.22$ in agreement with previous results of ST03. During both secular evolution and fusion, the bulges grow in mass and the potential wells get more concentrated at a 3σ level. Table 2 summarizes the variation in the parameters and residuals. To summarize, secular evolution seems to contribute to form a bulge component and to diminish the residuals of the Fundamental Mass Plane relation as the bulge gets in place.

To improve our understanding of the changes occurring during secular evolution phases, we plot the FP parameters against the structural ones at the redshifts of interest. Figure 6 shows log $r_{\rm eff}$ versus log σ_0 and $\Sigma_{\rm eff}$ (the so-called Kormendy relation). In terms of the relation log $r_{\rm eff}$ versus log σ_0, systems experiencing DSBs finish the merger events with a much steeper slope: dlog $r_{\rm eff}$/dlog $\sigma_0 \approx -2.25 \pm 1.15$, while they have dlog $r_{\rm eff}$/dlog $\sigma_0 \approx -0.90 \pm 0.19$ at the beginning of the merger event (Fig. 6a). In this case, fusions seem to contribute to the steepness of the slope so that, at a given $r_{\rm eff}$, the simulated discs have larger central velocity dispersion after the fusion. In the case of SSB events, the systems show an anti-correlation signal

with dlog $r_{\rm eff}$/dlog $\sigma_0 \approx -1.38 \pm 0.30$, which is not affected by the fusion (Fig. 6c).

Finally, the simulated Kormendy relation for systems experiencing DSBs adopts the observed slope (Table 1) after the secular evolution period, which produces a change from dlog $r_{\rm eff}$/d$\Sigma_{\rm eff}$ = 0.09 $\pm$ 0.02 at $z_{\rm A}$ to dlog $r_{\rm eff}$/d$\Sigma_{\rm eff}$ = 0.16 $\pm$ 0.03 at $z_{\rm C}$ (Fig. 6b). In the case of bulges during SSBs, the correlations are in place with the observed slope when the interactions start (Fig. 6d) with dlog $r_{\rm eff}$/d$\Sigma_{\rm eff}$ = 0.14 $\pm$ 0.04. The ODP or the fusion events do not modify them.

Hence, in these simulations, it is secular evolution that modifies the structural parameters in such a way that their combination produces a FP mass relation with the observed slope.

3.3. The Tully-Fisher mass relation for GLOs

Considering that the simulated bulges show structural parameters in agreement with those observed and that mergers contribute to establish their fundamental relations, we would like to analyze whether the fundamental relation for the disc components can be directly linked to the bulge ones. For this purpose, we will study the TF mass relation during merger events. We have fitted a linear regression to the data of McArthur et al. (2003) which comprise 304 nearby late-type (Sb-Sc) spiral galaxies in the R band,

$$M_R = -6.36 \cdot [\log\ v_{2.2{\rm r_d}} - 2.5] - 21.5, \qquad (3)$$

where $v_{2.2{\rm r_d}}$ is the velocity in km s^{-1} measured at 2.2$r_{\rm d}$. The magnitudes (M_R) of the GLOs are obtained assuming a constant mass-to-light ratio of $\Gamma = 7$ for the total baryonic mass, which provides a consistent zero point for the $z = 0$ relation. This ratio has been kept constant at all redshifts.

Taking into account the results found for the bulges, we focus on the analysis of the effects of fusions and secular evolution on the TF relation. In Fig. 7, we plot the TF relation for systems undergoing DSBs (upper panel) and SSBs (lower panel) at the redshifts of interest (i.e., $z_{\rm A}, z_{\rm C}, z_{\rm D}$). Interestingly, we found

that the TF relation behaves in a similar fashion to the FP relation (see Fig. 5). Those systems that experience secular evolution start systematically at a fainter magnitude than that predicted by the observed local TF relation for a given velocity. After secular evolution, a larger fraction of the simulated discs are consistent with the observed relation, are more concentrated, and move along the relation toward larger velocities and brighter magnitudes. Fusions introduce scatter and help to displace the discs further in the same direction. In the case of systems undergoing SSB events, they all show a TF relation in agreement with observations. Fusions tend to displace the systems along the TF relation toward higher velocities and brighter magnitudes, on average. Again, we found that when a system is stable during an orbital decay phase, it already has structural parameters that satisfy the fundamental relations for both the bulge and disc components.

The cross-correlation of the parameters of the TF and the FP relations reveals that as discs grow in magnitudes (i.e., masses) and circular velocities, the bulges get more concentrated. In particular, unstable systems (i.e., those experiencing secular evolution) have systematically less concentrated bulges and smaller discs. Large discs grow as the bulge gets concentrated. Our results point to a coupled formation of both components, suggesting a feedback process between them.

4. Discussion and conclusions

We have analyzed bulge-disc systems formed in hierarchical clustering scenarios, finding that their structural parameters agree with those of late-type bulges of spirals. We use the bulge-disc decomposition of the projected mass profiles to quantify *changes in the mass distribution during mergers*. The formation of systems with observational counterparts is obtained by adopting an inefficient star formation which allows the formation of compact bulges without exhausting the gas reservoir at early stages of evolution. In this scenario, mergers do not completely destroy the discs, but a remnant survives, leading to the formation of extended systems (Domínguez et al. 1998). Recently, Springel & Hernquist (2004) have shown that a correct modeling of the multiphase character of the interstellar medium produces similar results. Our simulations used a phenomenological and simple scheme which allows us to reproduce systems with observational counterparts and help to understand their evolution during mergers.

Note that our main aim is to study the changes during mergers and how GLOs get to the relation at $z = 0$ depending, on their evolutionary histories. For the sake of simplicity, a constant mass-to-light ratio is assumed for all redshifts, since we are interested in the analysis of the mass distributions. We have kept those values for all redshifts so that we can assess the departures from the local relations during violent events due to mass redistribution.

We have analyzed a higher numerical resolution run performed with Gadget-2, improving the resolution of baryons by one order of magnitude. We found similar trends in agreement with previous results from Domínguez et al. (1998). This test proves that the formation of galactic systems with the characteristics described in this paper is independent of the code used and is not determined by numerical artifacts.

The following items summarize our results:

- The simulated bulges have a Kormendy mass relation with a slope in agreement with observations at any redshift. However, when systems are segregated according to their internal properties, unstable systems (i.e., those that suffer double starbursts) determine a shallower relation. The combination of systems at different stages of evolution with different properties still yields a relation with the correct slope, but with a larger dispersion.

- The simulated bulges show an anticorrelation between the shape parameter n and the central surface density Σ_b^o in agreement with observations. Simulated bulges at $z = 0$ are situated at the faint end of the observed relation for intermediate and early-type spirals.

- At $z = 0$, the simulated bulges define a Fundamental Mass Plane with a slope consistent with observations, assuming a constant mass-to-light ratio. Their progenitors show a larger scatter. During gas-rich merger events, unstable systems (i.e., those that undergo secular evolution during their orbital decay phase) are located above the Fundamental Mass Plane at $z = 0$. After the secular evolution phase, they are situated closer to the Fundamental Mass Plane relation at 3σ level. Fusions increase the scatter along the observed relation, but do not significantly change it.

- We found that the parameters of the TF mass relation are correlated with those of the Fundamental Mass Plane in the sense that as the disc grows, the bulge gets more concentrated.

By analyzing the changes in the mass distribution of galactic systems during merger events, we found that secular evolution phases play an important role in the determination of a Fundamental Mass Plane with a slope in agreement with that of the observed luminosity FP. During these phases, gas inflows are driven, triggering strong star formation. In this way, compact stellar bulges are formed, and there is an increase in the mass concentration and velocity dispersion. We detect that the Kormendy relation for systems before experiencing secular evolution is shallower than the observed one, and the slope of the FP relation tends to be steeper. After the secular phase, the simulated Kormendy relation and the Fundamental Mass Plane reproduce the observed slope. The same behavior can be observed between $r_{\rm eff}$ and σ_0, so that after secular evolution, the bulges have higher central velocity dispersion. Those mergers that are not able to trigger gas inflows during the orbital decay phase involve systems with well-formed bulges and with structural parameters that already determine relations with observational counterparts. Taking into account previous works and, in particular, that of Bender et al. (1992), our findings suggest that secular evolution seems to be a necessary phase for the determination of a Fundamental Mass Plane with a slope in agreement with that observed for the luminosity FP. In this sense, the different position of compact and bright dE on the FP could be in agreement with the idea that the departure of bright dwarf galaxies might indicate a lack of an important secular evolution phase in their history of formation. Note that, in our simulations, systems get to the local fundamental relations at different stages of evolution so that the fundamental relations at a given redshift are the result of the contributions of systems at different epochs of formation. Hence, these differences in the merger histories introduce a natural dispersion in the relations (see also Kobayashi 2005). Finally, we should note that we have mimiced the effects of SN feedback in the regulation of the star formation activity by using a low star formation efficiency. Our results should be confirmed by models with self-consistent SN feedback treatment.

References

Andredakis, Y. C., Peletier, R. F., & Balcells, M. 1995, MNRAS, 275, 874
Athanassoula, E., & Sellwood, J. A. 1986, MNRAS, 221, 213
Barnes, J. E., & Hernquist, L. 1991, ApJ, 370, L65
Barnes, J. E., & Hernquist, L. 1992, ARA&A, 30, 705
Barnes, J. E., & Hernquist, L. 1996, ApJ, 471, 115
Bender, R., Burstein, D., & Faber, S. M. 1992, AJ, 399, 462
Binney, J., & Tremaine, S. 1987, Galactic Dynamics (Princeton, NJ: Princeton Univ. Press)
Capelato, H. V., de Carvalho, R. R., & Carlberg, R. G. 1995, ApJ, 451, 525
Christodoulou, D. M., Shlosman, I., & Tohline, J. E. 1995, ApJ, 443, 551
Cole, S., Lacey, C. G., Baugh, C. M., & Frenk, C. S. 2000, MNRAS, 319, 168
Courteau, S., de Jong, R., & Broeils, A. 1996, ApJ, 457, L73
Domínguez-Tenreiro, R., Tissera, P. B., & Sáiz, A. 1998, ApJ, 508, L123
Evrard, A. E., Summers, F. J., & Davis, M. 1994, ApJ, 422, 11
Evstigneeva, E. A., de Carvalho, R. R., Ribeiro, A. L., & Capelato, H. V. 2003, Ap&SS, 284, 487
Falcón-Barroso, J., Peletier, R. F., & Balcells, M. 2002, MNRAS, 335, 741 (FBPB02)
Fall, S. M., & Efstathiou, G. 1980, MNRAS, 193, 189
Khosroshahi, H. G., Wadadekar, Y., Kembhavi, A., & Mobasher, B. 2000a, ApJ, 531, L103
Khosroshahi, H. G., Wadadekar, Y., & Kembhavi, A. 2000b, ApJ, 533, 162 (K00b)
Kobayashi, C. 2005, MNRAS, 361, 1216
Kormendy, J. 1977, ApJ, 218, 333
Lacey, C., Guiderdoni, B., Rocca-Volmerange, B., & Silk, J. 1993, ApJ, 402, 15
MacArthur, L. A., Courteau, S., & Holtzman, J. A. 2003, ApJ, 582, 689
Martinet, L. 1995, Fund. Cosmic Phys., 15, 341

Mihos, J. C., & Hernquist, L. 1994, ApJ, 425, L13
Mihos, J. C., & Hernquist, L. 1996, ApJ, 464, 641
Mo, H. J., Mao, S., & White, S. D. M. 1998, MNRAS, 295, 319
Möllenhoff, C., & Heidt, J. 2001, A&A, 368, 16
Navarro, J. F., & Benz, W. 1991, ApJ, 380, 320
Navarro, J. F., & White, S. D. M. 1994, MNRAS, 267, 401
Navarro, J. F., & Steinmetz, M. 1997, ApJ, 478, 13
Navarro, J. F., Frenk, C. S., & White, S. D. M. 1995a, MNRAS, 275, 56
Navarro, J. F., Frenk, C. S., & White, S. D. M. 1995b, MNRAS, 275, 720
Pérez, M. J., Tissera, P. B., Lambas, D. G., & Scannapieco, C. 2006, A&A, 449, 23
Sáiz, A., Domínguez-Tenreiro, R., Tissera, P. B., & Courteau, S. 2001, MNRAS, 325, 119
Scannapieco, C., & Tissera, P. B. 2003, MNRAS, 338, 880 (ST03)
Scannapieco, C., Tissera, P. B., White, S. D. M., & Springel, V. 2005, MNRAS, 364, 552
Scannapieco, C., Tissera, P. B., White, S. D. M., & Springel, V. 2006, Proceedings for the Vth Marseille International Cosmology Conference: The Fabulous Destiny of Galaxies, in press [arXiv:astro-ph/0509440]
Sérsic, J. L. 1968, Atlas de Galaxias Australes, Observatorio Astronómico de Córdoba
Springel, V., & Hernquist, L. 2005, ApJL, submitted
Steinmetz, M., & White, S. D. M. 1997, MNRAS, 288, 545
Sommer-Larsen, J., Gelato, S., & Vedel, H. 1999, ApJ, 519, 501
Thacker, R. J., & Couchman, H. M. P. 2000, ApJ, 555, L17
Tissera, P. B. 2000, ApJ, 534, 636
Tissera, P. B., Lambas, D. G., & Abadi, M. G. 1997, MNRAS, 286, 384
Tissera, P. B., Domínguez-Tenreiro, R., Scannapieco, C., & Sáiz, A. 2002, MNRAS, 333, 327
Tissera, P. B., Scannapieco C., White, S. D. M., & Springel, V. 2006, Rev. Mex. Ast. Conf. Ser., in press [arXiv:astro-ph/0603633]
van den Bosch, F. C. 1998, ApJ, 507, 601
van den Bosch, F. C. 2000, ApJ, 530, 177
Vedel, H., Hellsten, U., & Sommer-Larsen, J. 1994, MNRAS, 271, 743
Weil, M. L., Eke, V. R., & Efstathiou, G. 1998, MNRAS, 300, 773
White, S. D. M., & Rees, M. J. 1978, MNRAS, 183, 341